

7,8-Dihydroxycoumarin Alleviates Synaptic Loss by Activated PI3K-Akt-CREB-BDNF Signaling in Alzheimer's Disease Model Mice

Li Yan,^{*,†} Yufan Jin,[†] Junping Pan, Xiang He, Shiqian Zhong, Rongcai Zhang, LokLam Choi, Weiwei Su,^{*} and Jiayu Chen^{*}

 Cite This: *J. Agric. Food Chem.* 2022, 70, 7130–7138

 Read Online

ACCESS |

 Metrics & More

 Article Recommendations

ABSTRACT: Alzheimer's disease (AD) is a progressive neurodegenerative disorder and is clinically characterized by the impairment of memory and cognition. Accumulation of β -amyloid ($A\beta$) in the brain is considered as a key process in the development of AD because it impairs the synapses' function to impair memory formation. Recent research studies have indicated that a group of edible plant-derived *Thymelaeaceae* compounds known as coumarin may exert particularly powerful actions on alleviating learning and memory impairment. 7,8-Dihydroxycoumarin (7,8-DHC), a bioactive component of coumarin derived from *Thymelaeaceae*, showed its function in neuroprotection before. In this study, we found that 7,8-DHC was able to mitigate $A\beta$ accumulation via reducing the level of BACE1 and increasing the level of ADAM17 and ADAM10. More importantly, we found that 7,8-DHC could mitigate memory impairment, promote the dendrite branch density, and increase synaptic protein expression via activating PI3K-Akt-CREB-BDNF signaling. Hence, these results suggested that 7,8-DHC represented a novel bioactive therapeutic agent in mitigating $A\beta$ deposition and synaptic loss in the process of treating AD.

KEYWORDS: Alzheimer's disease, 7,8-dihydroxycoumarin, synaptic loss, PI3K-Akt-CREB-BDNF, memory impairment

INTRODUCTION

Alzheimer's disease (AD), a progressive neurodegenerative disorder, is clinically characterized by the dysfunction of memory and cognition.¹ The pathology of AD is characterized by massive neuronal death in the brain, structural changes in brain tissues, and atrophy.² At present, several hypotheses are there to explain the AD pathology, such as β -amyloid ($A\beta$) aggregation, neurofibril tangles (NFTs), synaptic dysfunction, imbalance of calcium homeostasis, and inflammation. Especially, the $A\beta$ aggregation receives the most attention.³ Massive $A\beta$ deposition plays a key feature in AD because it may trigger following cascade events like synapse dysfunction and finally leads to brain damage and memory loss.^{4–6}

cAMP-response element binding protein (CREB) has been recently involved in several brain pathological conditions including cognitive and neurodegenerative disorders and can be activated by PI3K-Akt, MAPK, and JAK-STAT signaling. The $A\beta$ peptide playing an essential role in the pathogenesis of AD can alter synaptic plasticity and memory and mediates synaptic loss through the CREB.⁷ Altering CREB signaling has been observed in other cognitive disorders like Huntington's disease and amyotrophic lateral sclerosis, suggesting a crucial role of CREB signaling in synapse function.^{8,9}

Besides, activation of CREB enables the transcription of crucial proteins for synapse, particularly brain-derived neurotrophic factor (BDNF). BDNF is an essential mediator in synaptic transmission and long-term potential. Reduction of the level of BDNF may lead to the collapse of specific neuronal structures and progressive atrophy of neurons in the AD brain.^{10,11}

Medicinal herbs and natural products are an essential source of protection against AD. Coumarin is found in different plant sources such as vegetables, spices, fruits, and medicinal plants, showing strong biological activity in the central nervous system. Umbelliferone is an example that shows its neuroprotective effects in AD.¹² 7,8-Dihydroxycoumarin (7,8-DHC) is a natural coumarin component with a molecular weight of 178.14. It is isolated from common edible plants of the *Thymelaeaceae* family including *Daphne Korean Nakai*, *Daphne genkwa*, *Daphne odora*, *Daphne oleoides*, and so on. Previous studies suggested that 7,8-DHC can penetrate through the brain blood barrier and has multiple biological activities in neuroprotective, anti-parasitic, anti-arthritis, anti-hypoxia, and anti-proliferative aspects.^{13–17} Especially in neuroprotection, 7,8-DHC can increase MAP2 content in rat neurons and increase the dendrite length of cortical neurons cultured in vitro. It can also promote the expression of BDNF, which works as a protector in neurons.¹⁸

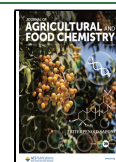
In this study, we verified that 7,8-DHC could reduce the deposition of $A\beta_{1-42}$ and mitigate memory impairment and synaptic loss. Then, the transcriptome results identified that 7,8-DHC could regulate PI3K-Akt-CREB-BDNF signaling as

Received: March 28, 2022

Revised: May 15, 2022

Accepted: May 18, 2022

Published: June 3, 2022



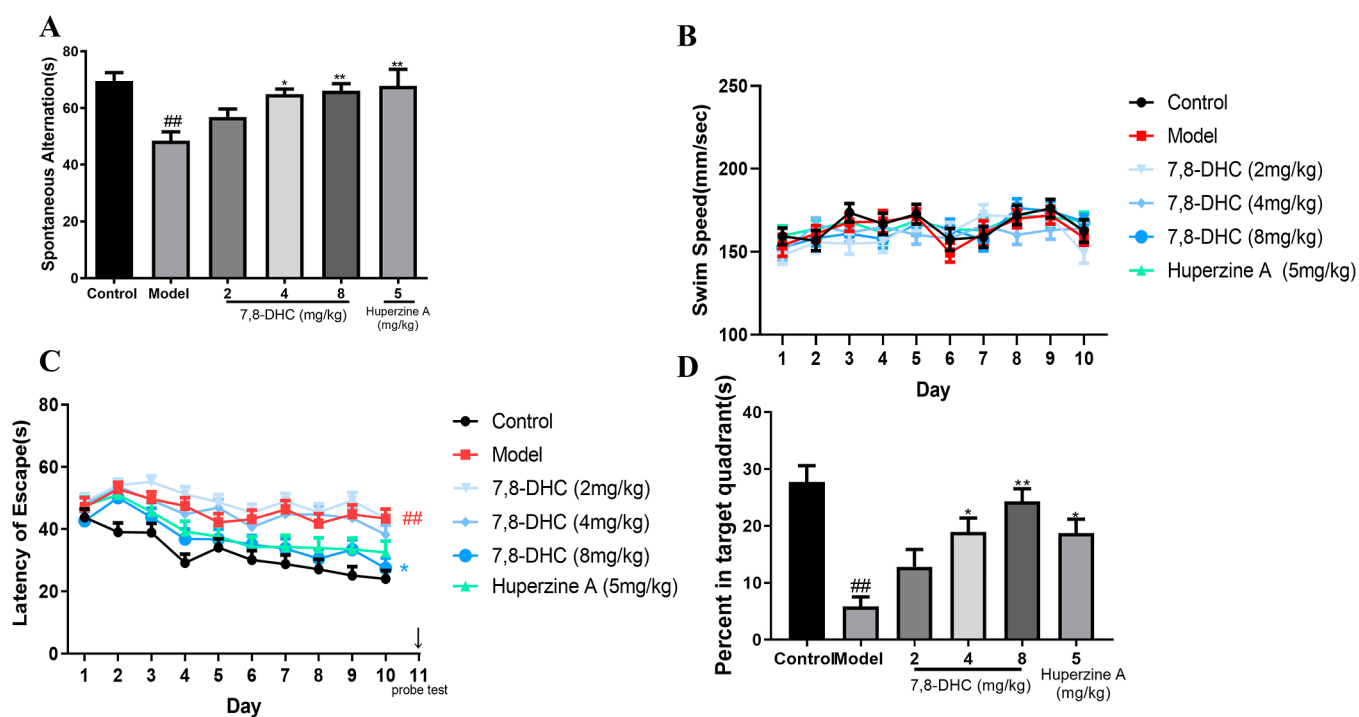


Figure 1. 7,8-DHC improved spatial learning and memory ability of 5x FAD mice. (A) Mice were tested in the Y-maze at the age of 7 months and assessed by spontaneous alternation. (B) Swim speed during escape latency. (C) Escape latency in the hidden platform during Morris water maze task training. (D) Time spent in the quadrant with the hidden platform during the probe trial. Data are presented as mean \pm SD and analyzed with one-way ANOVA in the Y-maze test and probe trial during the Morris water maze test; two-way ANOVA was performed in latency during the Morris water maze test. [#] $p < 0.05$ and ^{##} $p < 0.01$ compared with the control group, ^{*} $p < 0.05$ and ^{**} $p < 0.01$ compared with the model group, $n = 12$ mice per group.

the potential pathway to alleviate the symptom of AD, and finally, we confirmed it.

MATERIALS AND METHODS

Mice. 5x FAD transgenic mice expressing human *APP* and *PSEN1* with a total of five AD-linked mutations were raised in the SPF houses of Jinan University (license no. SYXK-(Yue) 2017-0174). All experimental procedures were approved by the Animal Care and Use Committee of Jinan University (permission no. IACUC-2011208-01) and carried out in accordance with the National Institutes of Health Guide for the Care and Use of Laboratory Animals (NIH publication no. 8023, revised 1978). The offspring of (hybrid 5x FAD transgenic and non-transgenic (wild type, WT)) mice were identified by polymerase chain reaction (PCR) of mouse tail DNA. In this study, both males and females ($n = 12$ per group) were used and all mice were treated according to the guidelines of China for animal care. Animals were bred and kept in a temperature-controlled room at $20\text{ }^{\circ}\text{C} \pm 2\text{ }^{\circ}\text{C}$ and a 12/12 h light–dark cycle (light on at 8 a.m.). Food and water were available *ad libitum*.

The 7 month-old mice were divided into different administered groups by gavage once for 30 consecutive days. A total of 60 5x FAD mice were divided into the model group, 7,8-dihydroxycoumarin low-dose group (2 mg/kg/per day), medium-dose group (4 mg/kg/per day), high-dose group (8 mg/kg/per day), and Huperzine A (5 mg/kg/per day) group. A total of 12 WT mice were treated as the control group. The control group and the model group were treated with the same volume of saline. 7,8-DHC first dissolved in 1% DMSO and then dispersed in saline. The saline in the model group and control group had the same volume of DMSO as the treatment groups.

Primary Neuron Culture. Primary hippocampus neurons were prepared from embryonic day 17–18 (E17–18) of 5x FAD mice and WT mice. The pregnant female mice were terminally anesthetized. Embryos were taken out from the uterus, and their tails were cut down for further genotype identification. Primary hippocampus

neurons were enzymatically dissociated with papain and mechanically dispersed into single cells. Then, the dissociated neurons were plated onto 0.1 mg/mL poly-L-lysine (Sigma) coated six-well plates at a density of 1×10^6 cells/well. Primary neurons were maintained at $37\text{ }^{\circ}\text{C}$ in the neural basal medium supplied with 2% B27 (ThermoFisher), 0.5 mM glutamine (ThermoFisher), 100 units/mL penicillin (Gibco), and 100 $\mu\text{g}/\text{mL}$ streptomycin (Gibco). After cells were completely adherent, we divided cells into four groups: control group (WT mice treated with 0.1% DMSO), model group (5x FAD treated with 0.1% DMSO), 7,8-DHC group (5x FAD mice treated with $8\text{ }\mu\text{M}$ 7,8-DHC and 0.1% DMSO), and 7,8-DHC + LY294002 group (5x FAD treated with $8\text{ }\mu\text{M}$ 7,8-DHC, $10\text{ }\mu\text{M}$ LY294002, and 0.1% DMSO). The culture medium with or without treatment was changed every second day. After incubation for 12 days, we collected all cells and detected the phosphorylation of PI3K, Akt, CREB, and the level of BDNF by western blot.

Morris Water Maze Test. Mice were trained to find an invisible 14 cm platform submerged 1.5 cm beneath the water surface. If a mouse could not find the platform within 60 s, it was manually guided to the platform and remained there for 30 s. The escape latency and swim speed were recorded for 60 s. Mice were given four trials per day. After the training period, each mouse received only one probe test that consisted of a 60 s free swim in the pool without the platform. The target quadrant was defined by the location where the hidden platform was previously placed in the hidden training session but removed during the probe test. An ANY-maze video tracking system was used to record all trials for automated analysis.

Y-Maze Test. Each mouse was placed in the center of the Y-maze. A single 5 min test was performed and recorded using a video camera. Arm entries and the order of entries are determined on recorded videos. Spontaneous alternations are defined and calculated as consecutive triplets of different arm choices.

Golgi Staining. Mice brains were dissected and treated with an FD Rapid GolgiStain Kit (FD Neuro Technologies, Shanghai, China) following the manufacturer's instruction. Slices were visualized under

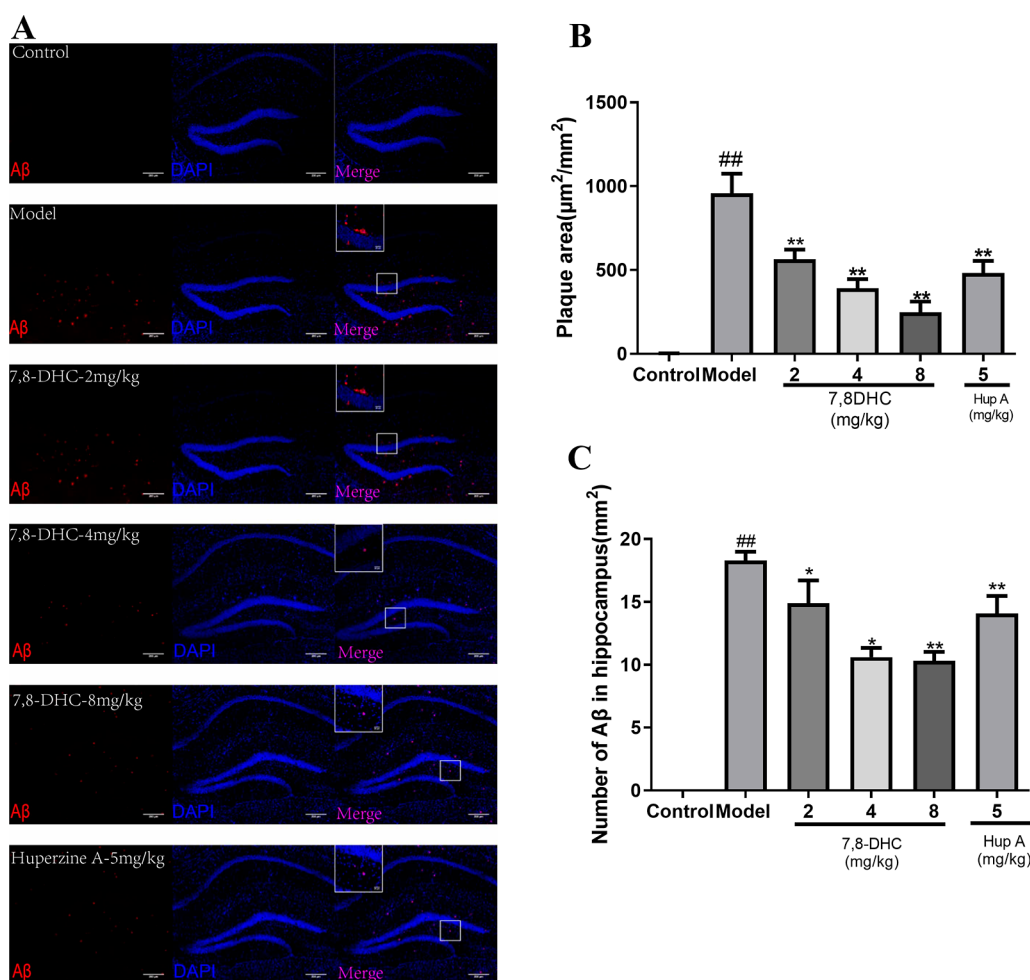


Figure 2. Treatment with 7,8-DHC can reduce the A β deposition in the hippocampus area. (A) Immunofluorescence staining analysis of A β in the control group, the model group, the different dosages of 7,8-DHC, and the Huperzine A group (magnification 100 \times). (B,C) Quantitative analysis of the number and volume of A β plaques in the hippocampi of the 7,8-DHC and Huperzine A groups. [#] $p < 0.05$ and ^{##} $p < 0.01$ compared with the control group, ^{*} $p < 0.05$ and ^{**} $p < 0.01$ compared with the model group (mean \pm SD, $n = 4$); scale bar: 100 μ m (one-way ANOVA).

a Nikon Confocal Microscope (Nikon, A1R HD25). Images were captured from Golgi-impregnated hippocampal CA1 pyramidal neurons. We counted the number of dendritic spines on projected deconvolved images.

Immunostaining. Mice were transcardially perfused with 4% paraformaldehyde (PFA) in PBS, and their brains were carefully dissected. Fixation was carried out in 4% PFA at 4 $^{\circ}$ C overnight and dehydrated with 10, 20, and 30% sucrose solution for 3 consecutive days. Brain slices for immunofluorescent staining were performed at a thickness of 20 μ m and subjected to immunostaining with rabbit anti-A β (1–42) IgG antibody (1:500) at 4 $^{\circ}$ C overnight. Then the brain slices were incubated with goat anti-rabbit Alex 594 antibody for 2 h at room temperature. Finally, the brain slices were mounted with DAPI Fluoromount-G. The images were taken on a Nikon Confocal Microscope.

Transcriptome Analysis. The RNA-seq technique was used to analyze the gene expression profiling with 7,8-DHC treatment. The cDNA fragments were purified using a QIAquick PCR extraction kit following the manufacturer's protocol. The cDNA fragments were enriched by PCR for construction of the cDNA library. The cDNA library was sequenced by an Illumina sequencing platform (IlluminaHiSeq 2500).

Western Blot Assay. Samples were lysed in RIPA buffer with phenylmethylsulfonyl fluoride and a protease inhibitor and then centrifuged at 18,000g at 4 $^{\circ}$ C for 20 min. BCA Protein Assay Reagent (Beyotime Biotechnology) was used to measure total protein concentration. Total protein (20 μ g) was boiled for 8 min in 5 \times

SDS loading buffer (Beyotime Biotechnology), separated by 10% SDS-polyacrylamide gel electrophoresis, and transferred to polyvinylidene difluoride (PVDF) membranes. Non-specific binding was prevented by incubating membranes in 5% nonfat milk dissolved in 1 \times Tris-buffered saline and Tween 20 (TBST) buffer at room temperature for 1 h. The membranes were incubated overnight at 4 $^{\circ}$ C with solutions of the primary antibody diluted with 1 \times TBST (anti-APP, 1:1000, CST; anti-BACE1, 1:1000, CST; anti-A β _{1–42}, 1:2000, CST; anti-ADAM10, 1:1000, CST; anti-PSEN1, 1:1000, CST; anti-ADAM17, 1:1000, CST; anti-phosph-Akt(ser473), 1:1000, CST; anti-Akt, 1:1000, CST; anti-PSD95, 1:1000, CST; anti-synaptophysin 1:1000, CST; anti-CREB, 1:1000, CST; anti-phosph-CREB(ser133), 1:1000, CST; anti-phosph-PI3K (p85(Tyr458)/p55(Tyr199)), 1:1000, CST; PI3K, 1:1000, CST; BDNF 1:1000, ABCAM). The membranes were washed and incubated with anti-mouse or anti-rabbit conjugated to horseradish peroxidase (HRP) (1:2500) at room temperature for 1 h before exposed in ECL solution (Millipore). The densitometry of protein was determined using a Gbox (Genetech).

Statistical Analysis. All the data were presented as mean \pm standard deviation (SD). Statistical analysis was performed using one-way ANOVA, followed by the least significant difference comparison test (more than two groups). The level of significance was set to p value < 0.05 . The ImageJ software was used for immunobiological quantitative analysis.

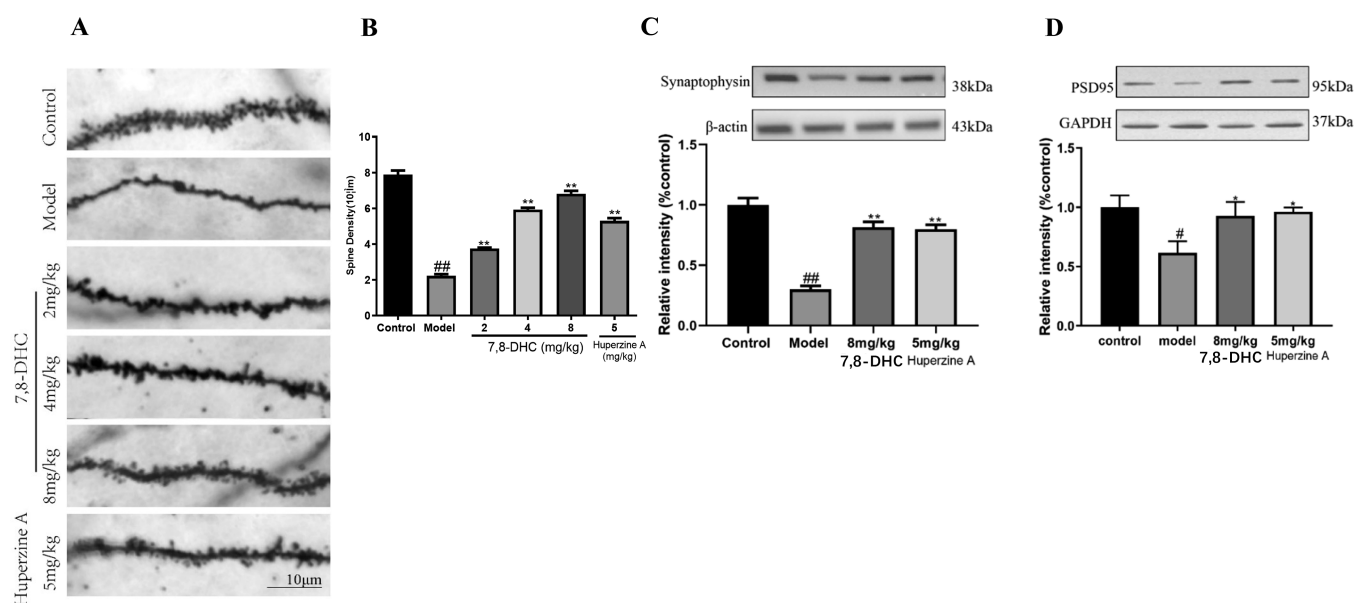


Figure 3. 7,8-DHC reversed synaptic impairment in 5XFAD mice. (A) Hippocampus regions from 7-month-old control, model, 2 mg/kg 7,8-DHC-treated, 4 mg/kg 7,8-DHC-treated, 8 mg/kg 7,8-DHC-treated, and Huperzine A-treated mice were subjected to Golgi stain. Scale bars = 20 mm. (B) Number of dendritic spines. (C) Level of synaptophysin. (D) Level of PSD95. Data are presented as mean \pm SD and analyzed with one-way ANOVA. [#] $p < 0.05$ and ^{##} $p < 0.01$ compared with the control group, ^{*} $p < 0.05$ and ^{**} $p < 0.01$ compared with the model group. $n = 15$ –25 neurons from four mice per group; $n = 4$ in immunoblotting.

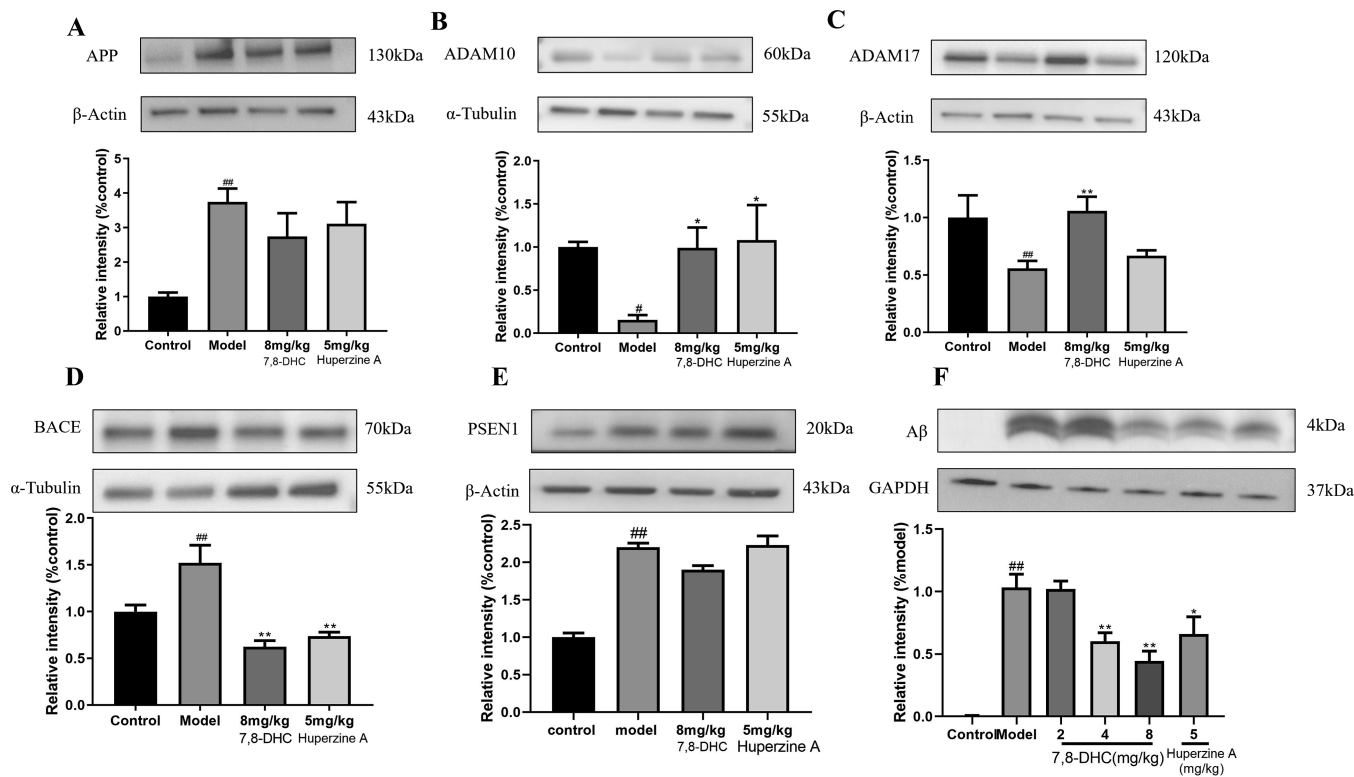


Figure 4. Effect of 7,8-DHC on reducing the level of A β via promoting α -secretase and decreasing β -secretase. (A) Level of APP; (B) Level of ADAM10; (C) level of ADAM17; (D) level of BACE; (E) level of PSEN1; (F) level of A β _{1–42}. [#] $p < 0.05$ and ^{##} $p < 0.01$ compared with the control group, ^{*} $p < 0.05$ and ^{**} $p < 0.01$ compared with the model group ($n = 3$ per group).

RESULTS

7,8-DHC Alleviated Cognitive Impairment in AD Mice. We performed Y-maze test to evaluate the effect of 7,8-DHC on mitigating cognitive impairment. From Figure 1A, model group mice showed a significant decrease in

spontaneous alternation compared to the control group ($p < 0.05$). However, spontaneous alternation was reversed after treatment with 7,8-DHC, especially 4 and 8 mg/kg treatment ($p < 0.05$), and did not differ from the Hup-A group. For evaluation of spatial memory, we performed the Morris water

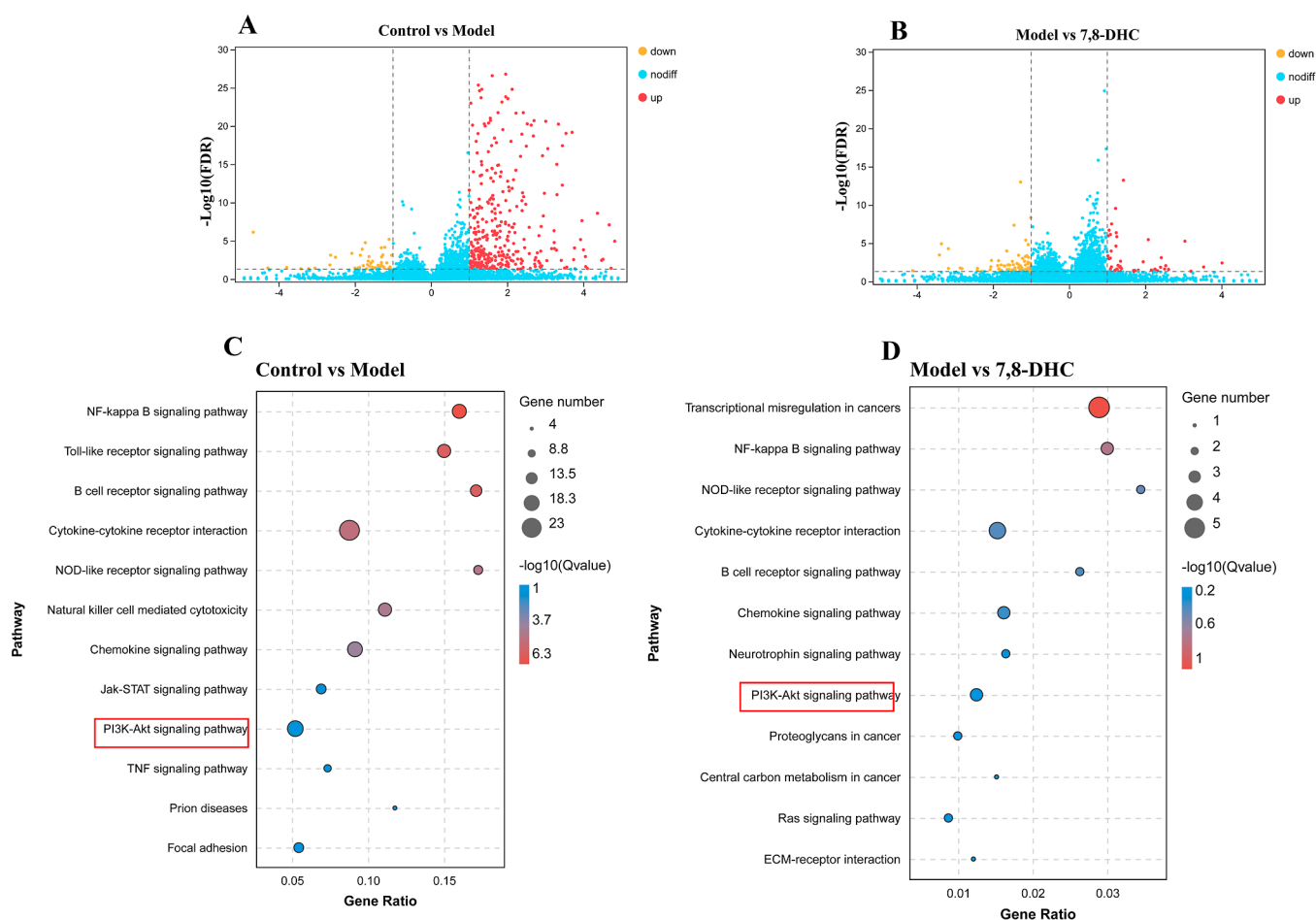


Figure 5. Transcriptomic analysis of 7,8-DHC on mitigation of synaptic loss. (A,B) Statistical result of all differentially expressed genes between control and model groups and model vs 7,8-DHC. (C) KEGG pathway enrichment of control and model groups. (D) KEGG pathway enrichment after the treatment of 7,8-DHC.

maze test. During the test period, all the mice did not show a difference in swimming speed (Figure 1B). During 10 days of training, model group mice demonstrated impaired spatial memory by spending longer times to find the hidden platform compared to the control group ($p < 0.01$), but the 8 mg/kg DHC group mice shortened their time to find the hidden platform ($p < 0.05$). Then, we removed the hidden platform and performed the probe test on the 11th day. Compared with the control group, the model group spent less time in the target quadrant. However, the 8 mg/kg 7,8-DHC group significantly spent a longer time than model groups ($p < 0.05$) and showed no difference with the Hup-A group. These results suggested that 7,8-DHC ameliorated memory dysfunction in 7-month-old 5×FAD mice (Figure 1C,D).

7,8-DHC Alleviated A β Deposition. We investigated the effects of 7,8-DHC on decreasing senile plaque formation in the 5×FAD mice hippocampus. The results in Figure 2 showed that the number and area of A β_{1-42} accumulation in the model group mice were significantly increased compared to the control group at 7 months of age ($p < 0.05$). Strikingly, the number and area of plaques in the hippocampus were significantly decreased in 7,8-DHC-treated mice in dosage when compared to the model group. The results indicated that 7,8-DHC reduced A β deposition ($p < 0.05$) in the hippocampal region.

7,8-DHC Can Increase the Dendrite Spine Density and the Level of Synaptic Proteins. Following behavioral analysis, we performed Golgi staining in the hippocampus to determine whether 7,8-DHC would confer neuroprotective effects to increase the dendrite spine density. Dendritic spine density was calculated from a single neuron dendrite branch in a 10 mm length of the hippocampus. The morphology of dendritic spines was abnormal in the model group (Figure 3A). According to Figure 3, the spine density was found to be significantly reduced in the model group compared to the control group ($p < 0.01$). However, with the treatment of 7,8-DHC, mice showed an increasing number of dendritic spines compared with model group mice ($p < 0.05$). These results suggest that 7,8-DHC increased the spine density under AD's pathological conditions.

Synaptic proteins are the main components for forming the structure of synapse. PSD95 and synaptophysin are the biomarkers of synapse. In our study, the levels of PSD 95 and synaptophysin are decreased significantly in the model group. However, we found that after treatment, 7,8-DHC could increase the level of PSD95 and synaptophysin, meaning that 7,8-DHC could help the formation of synapse or inhibit synaptic protein loss (Figure 3C,D).

7,8-DHC Attenuated A β Deposition via BACE1, ADAM10, and ADAM17. Modern research studies found that A β was a neurotoxic protein and its excessive

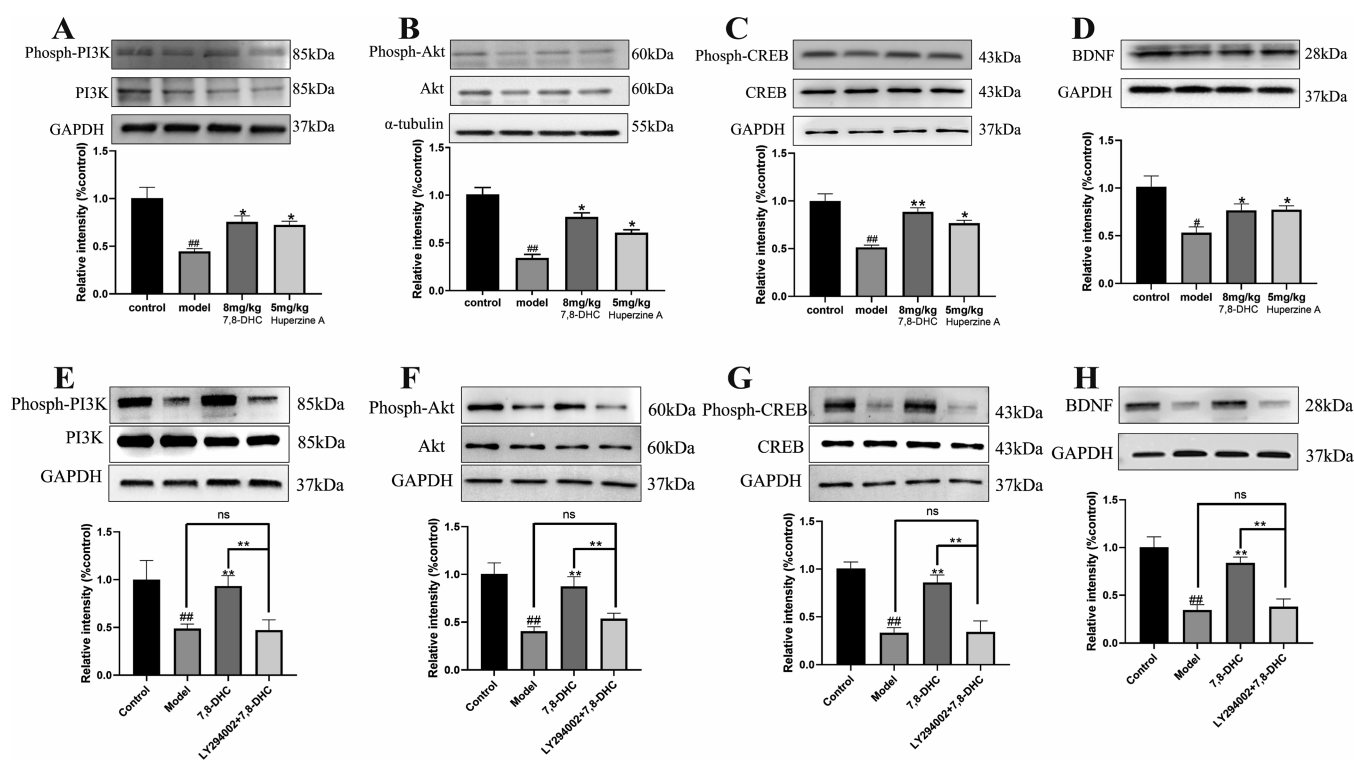


Figure 6. 7,8-DHC activated PI3K-Akt-CREB-BDNF signaling to reduce synaptic loss. (A–D) Phosphorylation level of PI3K, Akt, CREB, and the content of BDNF in the hippocampus area of mice's brain. (E–H) Phosphorylation level of PI3K, Akt, CREB, and the content of BDNF from primary neurons. # $p < 0.05$ and ## $p < 0.01$ compared with the control group, * $p < 0.05$ and ** $p < 0.01$ compared with the model group ($n = 3$ per group).

accumulation in the brain could lead to neuronal damage, neuron loss, and even neural network detriment. To determine how $A\beta$ deposition was reduced, we examined the expression of amyloid precursor protein (APP), disintegrin and metalloproteinase 10 and 17 (ADAM10 and ADAM17), β -site amyloid precursor protein cleaving enzyme 1 (BACE1), presenilin 1 (PSEN1), and $A\beta_{1-42}$ by western blot analysis. As shown in Figure 4A,E, the expressions of APP and PSEN1 in the hippocampus from the model group were strikingly more than those in the control group, in line with the feature of 5 \times FAD mice. ADAM10 and ADAM17, belonging to α -secretase, can cleave APP and preclude $A\beta$ formation. As shown in Figure 4B,C, in comparison to the control group, the ADAM10 and ADAM17 protein levels were decreased in the model group, but 7,8-DHC treatment increased the ADAM10 and ADAM17 protein levels. BACE1, belonging to β -secretase, played a key role in producing $A\beta$. The level of BACE1 from model group mice was extremely more than those in controls. However, 7,8-DHC decreased BACE1 levels compared to the model group (Figure 4D). As shown in Figure 4F, a number of $A\beta_{1-42}$ were observed in the hippocampus in model group mice. 7,8-DHC decreased the $A\beta_{1-42}$ level effectively in a dose-dependent manner. This result indicated that 7,8-DHC treatment could decrease the $A\beta_{1-42}$ level via upregulating α -secretase and downregulating β -secretase.

Transcriptome Sequencing Analysis of the Inhibition of Synaptic Loss Effects of 7,8-DHC. According to the effects of synaptic generation, we further explored the potential mechanism. The mRNA was collected for transcriptome sequencing analysis. Totally, we found 21,904 different expression genes. Differential genes between groups were calculated by edgeR. Compared with the control group, 404

genes were upregulated and 69 genes were downregulated in the model group. Compared with the model group, 68 genes were upregulated and 109 genes were downregulated in the 7,8-DHC treatment group (Figure 5A,B). Further, we found that 7,8-DHC might mainly activate PI3K-Akt signaling. PI3K-Akt signaling can also activate many downregulated components such as CREB, GSK3 β , and mTOR in protein generation, synaptic plasticity, and so on to exert its biological function (Figure 5C,D).

7,8-DHC Rescue Synaptic Loss via the PI3K-Akt-CREB-BDNF Pathway. The result of transcription indicated that 7,8-DHC might rescue synaptic loss by activating PI3K-Akt-CREB-BDNF signaling. Western blot was used to evaluate the mechanisms of 7,8-DHC-reduced synaptic loss. In the experiments in vivo, compared to control group mice, the level of the phosphorylation of PI3K, Akt, CREB, and the content of BDNF were less than those in the model group. However, 7,8-DHC treatment enhanced the levels of PI3K, Akt, and CREB phosphorylation and increased the content of BDNF (Figure 6A–D). Further, in the experiment in vitro, compared with the model group, the phosphorylation of PI3K, Akt, and CREB were increased and the level of BDNF also increased with the treatment of 8 μ M 7,8-DHC. After treating with LY294002 (the inhibitor of PI3K), these effects were inhibited by the PI3K inhibitor LY294002 (Figure 6E–H). The results suggested that 7,8-DHC could activate PI3K-Akt-CREB-BDNF signaling.

All the above results indicated that 7,8-DHC improves synaptic generation via activating PI3K-Akt-CREB-BDNF signaling (Figure 6).

DISCUSSION

AD is a typical age-related neurodegenerative disease and characterized by memory dysfunction.¹ Aggregation of A β peptide is believed to be a major cause of AD. The development of strategies to inhibit A β aggregation or increase A β degradation has received significant attention. 7,8-DHC, a plant-derivate edible component, showed its neuroprotective function in previous studies.¹⁸ In this study, we investigated the effect of 7,8-DHC on reducing memory impairment and synaptic loss in 5 \times FAD mice. We found that 7,8-DHC could mitigate the memory impairment by reducing A β deposition and promoting synaptic proteins in the hippocampal region. Further, 7,8-DHC could activate PI3K-Akt-CREB-BDNF signaling to enhance synaptic protein expression. A β deposition in the hippocampus leads to dysfunction of ion channels in neurons and disruption of intracellular calcium levels, inducing oxidative stress and causing abnormal energy and glucose metabolism, which in turn triggers neurotoxic and immunoinflammatory cascades.^{19–23} Therefore, reducing A β deposition is one of the important targets for AD treatment. Currently, several A β immunosuppressants are developed and investigated for their function in phase III clinical trials, such as MK-8931, ADUCAMUNAB, and ALBUMIN.^{24–26} The results of A β immunostaining in our study (Figure 2) showed that 7,8-DHC was able to reduce A β aggregation in 5 \times FAD mice hippocampi, suggesting that 7,8-DHC might work as a potential treatment candidate for AD.

Previous studies have also shown that A β deposition also damages the dendrite structure and reduces the content of synapse-associated proteins, leading to synaptic loss, disrupting neuronal networks, and ultimately leading to memory dysfunction.²⁷ In neuron morphological aspects, dendritic spines are tiny mushroom-like structures on dendrites and functional in synaptic plasticity and memory abilities.²⁸ The morphology of dendrite axes was thinner, and the density of dendritic spines was decreased in 5 \times FAD mice. However, after treatment of 7,8-DHC, the dendritic spine branched more and the axes became thicker than those in model group mice (Figure 3). We showed that 7,8-DHC can improve memory abilities in 5 \times FAD mice, as suggested by a higher spontaneous alternation in the Y-maze test, spending a longer time in the target quadrant, and less time escape latency in the Morris water maze test (Figure 1).

Synaptic loss is one of the pathological features of AD and is closely related to memory impairment.²⁹ The decrease of synaptic-related protein content is the main cause of synaptic loss and impaired synaptic functions. The presynaptic protein, synaptophysin, is associated with synaptic vesicle transport, docking, and release.³⁰ The postsynaptic membrane dense (PSD) is a hallmark component of postsynaptic membrane proteins, mainly composed of PSD95\synaptic GTPase-activating protein (syn-GAP) and the backbone protein, actin, which can help anchor glutamate receptors and their associated signaling proteins to the PSD region for signaling. PSD95 contributes to the formation of dendritic spines, which are important structures for the connection between neurons and are also the key sites for synapse formation.^{31,32} It was found that A β deposition could do harm to synaptophysin and PSD95 protein levels in the brains of 5 \times FAD mice,³³ while the present study showed that 7,8-DHC exerted actions on inhibiting synaptic protein loss (Figure 3). APP is sheared by α , β , and γ secretases to form different products. BACE1 is the

rate-limiting factor for A β production. sAPP β and C99 fragments are generated after APP is hydrolyzed by BACE1. Following this, C99 fragments are then cleaved by PSEN1 to generate A β fragments. If APP is cleaved by α -secretases, including ADAM10 and ADAM17, it would facilitate the generation of sAPP α and C83 fragments. In the following steps, C83 would be cleaved by PSEN1 to produce the p3 and AICD fragments, instead of A β fragments. 7,8-DHC reduced A β aggregation by decreasing β -secretase and increasing α -secretase expression, thereby reducing A β -mediated synaptic dysfunction and even improving cognitive dysfunction.^{34–36} In our study, the results indicated that 7,8-DHC can reduce the A β aggregation to ameliorate synapse dysfunction (Figure 4).

The transcriptome is developed to look for a potential mechanism to explain why the components work. Here, we found that 7,8-DHC might work by activating PI3K-Akt signaling. PI3K-Akt signaling can be activated through receptor tyrosine kinases (RTKs) or G protein-coupled receptors (GPCRs) and plays a crucial role in regulating survival and anti-apoptosis.³⁷ Activation of Akt through phosphorylation at Ser473 inhibits the transcription factor of apoptosis and promotes cell survival. CREB is a regulatory component in the nucleus of eukaryotic cells that plays an important regulatory role in the nervous system, promoting neuronal survival, increasing neural protrusions, and promoting neuronal differentiation.^{38,39} In addition, CREB transcription is related to learning and memory and can activate downstream genes by interacting with various molecular chaperones as well as promote synaptic protein synthesis.^{40,41} BDNF facilitates the transport of mRNAs along dendrites and their translation at the synapse by modulating the initiation and elongation in long-term changes.⁴² An altered expression level of BDNF might lead to synapse and memory loss in the AD brain. Increasing expression of BDNF by modulating of levels of CREB can increase the level of PSD95 and save patients from memory deficits as well as cognitive dysfunction.¹⁰ In neurons, the increase of BDNF by PI3K-Akt-CREB could augment synaptic protein formation and alleviate the symptoms of AD.⁴³ Our results suggested that 7,8-DHC activates PI3K-Akt-CREB signaling to promote BDNF expression to inhibit synaptic loss induced by A β overproduction (Figure 6).

In conclusion, we found that 7,8-DHC can alleviate the symptoms of AD. It can inhibit the overproduction of A β by reducing the content of BACE1 and increase the level of ADAM17 and ADAM10. Furthermore, it can inhibit synaptic loss through activation of the PI3K-Akt-CREB-BDNF pathway.

AUTHOR INFORMATION

Corresponding Authors

Li Yan – Formula-Pattern Research Center, School of Traditional Chinese Medicine, Jinan University, Guangzhou 510632, China; orcid.org/0000-0001-7232-8353; Phone: +86-02085221543; Email: liyan@jnu.edu.cn

Weiwei Su – Guangdong Engineering & Technology Research Center for Quality and Efficacy Reevaluation of Post-Market Traditional Chinese Medicine, Guangdong Key Laboratory of Plant Resources, School of Life Sciences, Sun Yat-sen University, Guangzhou 510275, China; orcid.org/0000-0002-1303-6331; Phone: +86-20-8411-2398; Email: lssww@126.com

Jiaxu Chen – Formula-Pattern Research Center, School of Traditional Chinese Medicine, Jinan University, Guangzhou

510632, China; Phone: +86-010-64286656;

Email: chenjiayu@hotmail.com

Authors

Yufan Jin – Guangdong Engineering & Technology Research Center for Quality and Efficacy Reevaluation of Post-Market Traditional Chinese Medicine, Guangdong Key Laboratory of Plant Resources, School of Life Sciences, Sun Yat-sen University, Guangzhou 510275, China

Junping Pan – Department of Pharmacology, School of Basic Medicine, Jinan University, Guangzhou 510632, China

Xiang He – Guangdong Engineering & Technology Research Center for Quality and Efficacy Reevaluation of Post-Market Traditional Chinese Medicine, Guangdong Key Laboratory of Plant Resources, School of Life Sciences, Sun Yat-sen University, Guangzhou 510275, China

Shiqian Zhong – International School, Jinan University, Guangzhou 510632, China

Rongcai Zhang – International School, Jinan University, Guangzhou 510632, China

LokLam Choi – International School, Jinan University, Guangzhou 510632, China

Complete contact information is available at:

<https://pubs.acs.org/10.1021/acs.jafc.2c02140>

Author Contributions

¹L.Y. and Y.J. contribute equally to this work.

Funding

This research was supported by grants from the Huang Zhendong Research Fund for Traditional Chinese Medicine of Jinan University, the National Science Foundation for Young Scientists of China (grant no. 81903617), and the Postdoctoral Science Foundation of China (no. 2021M691259).

Notes

The authors declare no competing financial interest.

ACKNOWLEDGMENTS

We would like to thank Formula-Pattern Research Center, School of Traditional Chinese Medicine, Jinan University.

ABBREVIATIONS

AD, Alzheimer's disease; Akt, protein kinase B; A β , β -amyloid; 7,8-DHC, 7,8-dihydroxycoumarin; ADAM17, disintegrin and metalloproteinase 17; ADAM10, disintegrin and metalloproteinase 10; PI3K, phosphoinositide 3-kinase; CREB, cAMP-response element binding protein; BACE1, beta-site amyloid precursor protein cleaving enzyme 1; PSEN, presenilin-1; APP, amyloid protein precursor; BDNF, brain-derived neurotrophic factor

REFERENCES

- (1) Montine, T. J.; Phelps, C. H.; Beach, T. G.; Bigio, E. H.; Cairns, N. J.; Dickson, D. W.; Duyckaerts, C.; Frosch, M. P.; Masliah, E.; Mirra, S. S.; Nelson, P. T.; Schneider, J. A.; Thal, D. R.; Trojanowski, J. Q.; Vinters, H. V.; Hyman, B. T. National Institute on Aging-Alzheimer's Association guidelines for the neuropathologic assessment of Alzheimer's disease: a practical approach. *Acta Neuropathol.* **2012**, *123*, 1–11.
- (2) Serrano-Pozo, A.; Frosch, M. P.; Masliah, E.; Hyman, B. T. Neuropathological alterations in Alzheimer disease. *Cold Spring Harbor Perspect. Med.* **2011**, *1*, a006189.
- (3) Frautschy, S. A.; Cole, G. M. Why pleiotropic interventions are needed for Alzheimer's disease. *Mol. Neurobiol.* **2010**, *41*, 392–409.

- (4) Tiwari, S.; Atluri, V.; Kaushik, A.; Yndart, A.; Nair, M. Alzheimer's disease: pathogenesis, diagnostics, and therapeutics. *Int. J. Nanomed.* **2019**, *14*, 5541–5554.

- (5) Naito, Y.; Tanabe, Y.; Lee, A. K.; Hamel, E.; Takahashi, H. Amyloid- β Oligomers Interact with Neurexin and Diminish Neurexin-mediated Excitatory Presynaptic Organization. *Sci. Rep.* **2017**, *7*, 42548.

- (6) Murphy, M. P.; LeVine, H., 3rd Alzheimer's disease and the amyloid-beta peptide. *J. Alzheimer's Dis.* **2010**, *19*, 311–323.

- (7) Saura, C. A.; Valero, J. The role of CREB signaling in Alzheimer's disease and other cognitive disorders. *Rev. Neurosci.* **2011**, *22*, 153–169.

- (8) Josselyn, S.; Nguyen, P. CREB, synapses and memory disorders: past progress and future challenges. *Curr. Drug Targets* **2005**, *4*, 481–497.

- (9) Saura, C. A.; Cardinaux, J.-R. Emerging Roles of CREB-Regulated Transcription Coactivators in Brain Physiology and Pathology. *Trends Neurosci.* **2017**, *40*, 720–733.

- (10) Amidfar, M.; de Oliveira, J.; Kucharska, E.; Budni, J.; Kim, Y.-K. The role of CREB and BDNF in neurobiology and treatment of Alzheimer's disease. *Life Sci.* **2020**, *257*, 118020.

- (11) Zarneshan, S. N.; Fakhri, S.; Khan, H. Targeting Akt/CREB/BDNF signaling pathway by ginsenosides in neurodegenerative diseases: A mechanistic approach. *Pharmacol. Res.* **2022**, *177*, 106099.

- (12) Guesne, S.; Connole, L.; Kim, S.; Motevalli, M.; Robson, L.; Michael-Titus, A. T.; Sullivan, A. Umbelliferoyloxymethyl phosphonate compounds-weakly binding zinc ionophores with neuroprotective properties. *Dalton Trans.* **2021**, *50*, 17041–17051.

- (13) Deng, Q.; Wu, L.; Li, Y.; Zou, L. Chemoprotective Effect of Daphnetin in Doxorubicin Treated Esophageal Cancer Stem Cell Xenograft Tumor Mouse. *Dokl. Biochem. Biophys.* **2021**, *499*, 273–281.

- (14) Du, G.; Tu, H.; Li, X.; Pei, A.; Chen, J.; Miao, Z.; Li, J.; Wang, C.; Xie, H.; Xu, X.; Zhao, H. Daphnetin, a natural coumarin derivative, provides the neuroprotection against glutamate-induced toxicity in HT22 cells and ischemic brain injury. *Neurochem. Res.* **2014**, *39*, 269–275.

- (15) Jiménez-Orozco, F. A.; Randelović, I.; Hegedüs, Z.; Vega-Lopez, A.; Martínez-Flores, F.; Tóvári, J. In vitro anti-proliferative effect and in vivo antitumor action of daphnetin in different tumor cells. *Cir. Cir.* **2020**, *88*, 765–771.

- (16) Wang, G.; Pang, J.; Hu, X.; Nie, T.; Lu, X.; Li, X.; Wang, X.; Lu, Y.; Yang, X.; Jiang, J.; Li, C.; Xiong, Y. Q.; You, X. Daphnetin: A Novel Anti-Helicobacter pylori Agent. *Int. J. Mol. Sci.* **2019**, *20*, 850.

- (17) Zhang, X.; Yao, J.; Wu, Z.; Zou, K.; Yang, Z.; Huang, X.; Luan, Z.; Li, J.; Wei, Q. Chondroprotective and antiarthritic effects of Daphnetin used in vitro and in vivo osteoarthritis models. *Life Sci.* **2020**, *240*, 116857.

- (18) Yan, L.; Zhou, X.; Zhou, X.; Zhang, Z.; Luo, H.-M. Neurotrophic effects of 7,8-dihydroxycoumarin in primary cultured rat cortical neurons. *Neurosci. Bull.* **2012**, *28*, 493–498.

- (19) Arispe, N.; Diaz, J. C.; Simakova, O. A β ion channels. Prospects for treating Alzheimer's disease with A β channel blockers. *Biochim. Biophys. Acta Biomembr.* **2007**, *1768*, 1952–1965.

- (20) Furst, A. J.; Lal, R. A. Amyloid- β and glucose metabolism in Alzheimer's disease. *J. Alzheimer's Dis.* **2011**, *26*, 105–116.

- (21) Han, X.-J.; Hu, Y.-Y.; Yang, Z.-J.; Jiang, L.-P.; Shi, S.-L.; Li, Y.-R.; Guo, M.-Y.; Wu, H.-L.; Wan, Y.-Y. Amyloid β -42 induces neuronal apoptosis by targeting mitochondria. *Mol. Med. Rep.* **2017**, *16*, 4521–4528.

- (22) Selkoe, D. J. Alzheimer's disease: genes, proteins, and therapy. *Physiol. Rev.* **2001**, *81*, 741–766.

- (23) Tönnies, E.; Trushina, E. Oxidative Stress, Synaptic Dysfunction, and Alzheimer's Disease. *J. Alzheimer's Dis.* **2017**, *57*, 1105–1121.

- (24) Tampi, R. R.; Forester, B. P.; Agronin, M. Aducanumab: evidence from clinical trial data and controversies. *Drugs Context* **2021**, *10*, 2021–2073.

- (25) Yamamoto, K.; Shimada, H.; Koh, H.; Ataka, S.; Miki, T. Serum levels of albumin-amyloid beta complexes are decreased in Alzheimer's disease. *Geriatr. Gerontol. Int.* **2014**, *14*, 716–723.
- (26) Yan, R.; Vassar, R. Targeting the β secretase BACE1 for Alzheimer's disease therapy. *Lancet Neurol.* **2014**, *13*, 319–329.
- (27) Buggia-Prévot, V.; Fernandez, C. G.; Udayar, V.; Vetrivel, K. S.; Elie, A.; Roseman, J.; Sasse, V. A.; Lefkowitz, M.; Meckler, X.; Bhattacharyya, S.; George, M.; Kar, S.; Bindokas, V. P.; Parent, A. T.; Rajendran, L.; Band, H.; Vassar, R.; Thinakaran, G. A function for EHD family proteins in unidirectional retrograde dendritic transport of BACE1 and Alzheimer's disease $A\beta$ production. *Cell Rep.* **2013**, *5*, 1552–1563.
- (28) Šišková, Z.; Justus, D.; Kaneko, H.; Friedrichs, D.; Henneberg, N.; Beutel, T.; Pitsch, J.; Schoch, S.; Becker, A.; von der Kammer, H.; Remy, S. Dendritic structural degeneration is functionally linked to cellular hyperexcitability in a mouse model of Alzheimer's disease. *Neuron* **2014**, *84*, 1023–1033.
- (29) Du, H.; Guo, L.; Yan, S.; Sosunov, A. A.; McKhann, G. M.; ShiDu Yan, S. Early deficits in synaptic mitochondria in an Alzheimer's disease mouse model. *Proc. Natl. Acad. Sci. U.S.A.* **2010**, *107*, 18670.
- (30) Derksen, M. J.; Ward, N. L.; Hartle, K. D.; Ivanco, T. L. MAP2 and synaptophysin protein expression following motor learning suggests dynamic regulation and distinct alterations coinciding with synaptogenesis. *Neurobiol. Learn. Mem.* **2007**, *87*, 404–415.
- (31) Chetkovich, D. M.; Bunn, R. C.; Kuo, S.-H.; Kawasaki, Y.; Kohwi, M.; Bredt, D. S. Postsynaptic targeting of alternative postsynaptic density-95 isoforms by distinct mechanisms. *J. Neurosci.* **2002**, *22*, 6415–6425.
- (32) Yao, W.-D.; Gainetdinov, R. R.; Arbuckle, M. I.; Sotnikova, T. D.; Cyr, M.; Beaulieu, J.-M.; Torres, G. E.; Grant, S. G. N.; Caron, M. G. Identification of PSD-95 as a regulator of dopamine-mediated synaptic and behavioral plasticity. *Neuron* **2004**, *41*, 625–638.
- (33) Oakley, H.; Cole, S. L.; Logan, S.; Maus, E.; Shao, P.; Craft, J.; Guillozet-Bongaarts, A.; Ohno, M.; Disterhoft, J.; Van Eldik, L.; Berry, R.; Vassar, R. Intraneuronal beta-amyloid aggregates, neurodegeneration, and neuron loss in transgenic mice with five familial Alzheimer's disease mutations: potential factors in amyloid plaque formation. *J. Neurosci.* **2006**, *26*, 10129–10140.
- (34) Asai, M.; Hattori, C.; Szabó, B.; Sasagawa, N.; Maruyama, K.; Tanuma, S.-i.; Ishiura, S. Putative function of ADAM9, ADAM10, and ADAM17 as APP alpha-secretase. *Biochem. Biophys. Res. Commun.* **2003**, *301*, 231–235.
- (35) Buxbaum, J. D.; Gandy, S. E.; Cicchetti, P.; Ehrlich, M. E.; Czernik, A. J.; Fracasso, R. P.; Ramabhadran, T. V.; Unterbeck, A. J.; Greengard, P. Processing of Alzheimer beta/A4 amyloid precursor protein: modulation by agents that regulate protein phosphorylation. *Proc. Natl. Acad. Sci. U.S.A.* **1990**, *87*, 6003–6006.
- (36) O'Brien, R. J.; Wong, P. C. Amyloid precursor protein processing and Alzheimer's disease. *Annu. Rev. Neurosci.* **2011**, *34*, 185–204.
- (37) Hers, I.; Vincent, E. E.; Tavaré, J. M. Akt signalling in health and disease. *Cell. Signal.* **2011**, *23*, 1515–1527.
- (38) Lee, M. M.; Badache, A.; DeVries, G. H. Phosphorylation of CREB in axon-induced Schwann cell proliferation. *J. Neurosci. Res.* **1999**, *55*, 702–712.
- (39) Lonze, B. E.; Riccio, A.; Cohen, S.; Ginty, D. D. Apoptosis, axonal growth defects, and degeneration of peripheral neurons in mice lacking CREB. *Neuron* **2002**, *34*, 371–385.
- (40) Ahmed, T.; Frey, J. Plasticity-specific phosphorylation of CaMKII, MAP-kinases and CREB during late-LTP in rat hippocampal slices in vitro. *Neuropharmacology* **2005**, *49*, 477–492.
- (41) Guzowski, J. F.; McGaugh, J. L. Antisense oligodeoxynucleotide-mediated disruption of hippocampal cAMP response element binding protein levels impairs consolidation of memory for water maze training. *Proc. Natl. Acad. Sci. U.S.A.* **1997**, *94*, 2693–2698.
- (42) Leal, G.; Comprido, D.; Duarte, C. B. BDNF-induced local protein synthesis and synaptic plasticity. *Neuropharmacology* **2014**, *76*, 639–656.
- (43) Yoshii, A.; Constantine-Paton, M. BDNF induces transport of PSD-95 to dendrites through PI3K-AKT signaling after NMDA receptor activation. *Nat. Neurosci.* **2007**, *10*, 702–711.